Anal. Bioanal. Electrochem., Vol. 17, No. 1, 2025, 67-84
https://www.doi.org/10.22034/abec.2025.720380

Analytical & Bioanalytical Electrochemistry

Full Paper

Electrochemical based Biosensor using Multi-layer ZnO Nanostructures for Direct Detection of Glucose

Sajjad Sanjari,[1] Javad Koohsorkhi,[1,*] and Mehdi Mehrpooya[2]

[1]*Advanced Micro and Nano Fabrication Devices Lab, Department of MEMS and NEMS, School of Intelligent Systems, College of Interdisciplinary Science and Technology, University of Tehran, Tehran, Iran*
[2]*School of Energy Engineering and Sustainable Resources, College of Interdisciplinary Science and Technology, University of Tehran, Tehran, Iran*

*Corresponding Author, Tel.: +98-9126771808
E-Mail: koohsorkhi@ut.ac.ir

Received: 26 December 2024 / Received in revised form: 27 January 2025 / Accepted: 28 January 2025 / Published online: 31 January 2025

Abstract- This article investigates an enzyme-based electrochemical biosensor for glucose detection using hydrothermal zinc oxide. To enhance sensitivity and accelerate electron transfer, multidimensional ZnO nanostructures were implemented within this electrochemical cell on a glass substrate. By employing zinc oxide nanostructures and various electrode configurations, sensitivity increased from 9.45 $\mu AmM^{-1}cm^{-2}$ to 21.12 $\mu AmM^{-1}cm^{-2}$. In this article, zinc oxide nanostructures were used in one-layered and multilayered manner, yielding sensitivities of 13.63 $\mu AmM^{-1}cm^{-2}$ and 21.12 $\mu AmM^{-1}cm^{-2}$, respectively. The sensor response is around 7.1 seconds and the device covers a valuable diagnostic range due to its low limit of detection and wide operational range (0.002–10 mM). Cyclic voltammetry (CV) and linear sweep voltammetry (LSV) were conducted for the biosensor both without and with the analyte. The maximum current peak observed at a scan rate of 200 mV/s at 60 mV was 70.06 µA for the sample coated with multilayered nanostructures of ZnO. These tests indicated that electron transfer via multilayer nanostructures was superior to that of single-layer nanostructures.

Keywords- Glucose biosensor; Glucose oxidase enzyme; Zinc oxide nanostructures; Amperometry; Cyclic voltammetry

1. INTRODUCTION

Electrochemical glucose biosensors represent a category of sensors in which the biological component (receptor) is a biorecognition element, while the electrode functions as a transducer, converting biological information into an electronic signal. The interaction between the analyte (the substance to be measured) and the bioreceptor results in the generation of an electrical signal (amperometric response, potentiometric response, etc.) proportional to the analyte concentration [1]. The history of glucose enzyme electrodes began in 1962 with the development of the first enzymatic glucose sensor using an electrochemical approach based on a thin film of glucose oxidase (GOx) by Clark and Lyons at Cincinnati Hospital. The enzyme catalyzed the oxidation of glucose in the presence of oxygen, which was then detected by a platinum cathode, serving as a signal for glucose measurement [2].

Electrochemical biosensors can be classified into two categories: catalytic (enzymatic) electrochemical biosensors, where the bioreceptor is an enzyme, cell, or tissue, and affinity biosensors, where antibodies, membrane receptors, or nucleic acids are immobilized on the electrode. Enzymes represent a significant category of proteins that catalyze biochemical reactions within biological systems. This group of catalysts exhibits high efficiency and selectivity [3].

Electrochemical biosensors for glucose detection are classified into three generations. The first generation operates based on the production, consumption, and detection of hydrogen peroxide. The second generation utilizes electron mediators, which transfer electrons from the enzyme's active site to the electrode surface upon oxidation and reduction. In the third generation, electron transfer occurs directly from the enzyme to the electrode surface. One of the challenges associated with first-generation biosensors is the interference caused by electroactive species, such as reduced endogenous substances like ascorbic and uric acids, along with some pharmaceuticals like acetaminophen [4]. The second generation employs a non-physiological electron acceptor, such as ferrocene derivatives or synthetic mediators, in place of oxygen. This synthetic mediator functions as a physiological electron acceptor, improving accuracy by addressing the deficiencies associated with oxygen. Carbon nanotubes and gold nanoparticles can bind to the enzyme, creating a favorable orientation on the surface and acting as electrical connectors between the enzyme's active site and the electrode surface [1,2].

Occasionally, artificial enzymes are used for stronger electron transfer [5]. One effective approach to enhance electrical communication with the electrode involves enzyme modification. Weilin and his team reported a precise method for modifying glucose oxidase with electron amplifiers, achieving effective electrical connectivity. For this purpose, the active center, FAD (flavin adenine dinucleotide), was removed to allow for the positioning of a ferrocene electron mediator prior to the reconstitution of the apoenzyme with the modified FAD [5]. The reduced form of the enzyme, upon oxidation at the electrodes, sends an electrical

signal proportional to glucose concentration, while the oxidized mediator is subsequently reduced.

In the third generation, mediator species are eliminated, resulting in reagentless biosensors with operating potentials close to the oxidation/reduction potential of the enzyme. In this setup, the electrode potential is more positive than the oxidation potential of glucose oxidase, allowing for the direct electron transfer from the enzyme's active site to the electrode surface. Most blood glucose monitors rely on screen-printed enzyme electrode test strips [1]. Figure 1 summarizes the various generations of amperometric glucose biosensors based on different electron transfer mechanisms, including natural secondary wafers, synthetic redox mediators, and direct electron transfer [2].

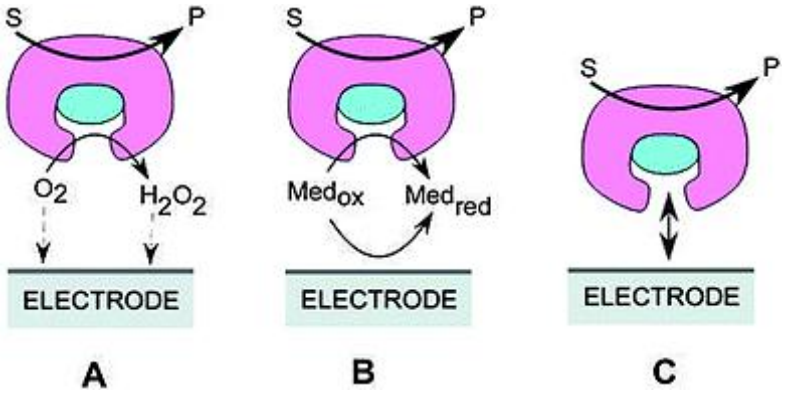

Figure 1. Three generations of amperometric enzyme electrodes for glucose: A) Natural oxygen cofactor, B) Artificial redox mediators, C) Direct electron transfer between glucose oxidase and the electrode [2]

Glucose oxidase catalyzes the oxidation of glucose to hydrogen peroxide and D-glucono-δ-Lactone, demonstrating an antibacterial reaction in the presence of oxygen and glucose oxidase [6]. Direct electron transfer from glucose oxidase to the surface of conventional electrodes is not possible because a thick protein layer surrounds the Flavin Adenine Dinucleotide (FAD) redox center, creating an inherent barrier to electron transfer. Therefore, one of the electron transfer techniques must be employed to facilitate the transfer of electrons from the enzyme's active center to the electrode surface [3].

In amperometric systems, the current flows between the counter and the working electrode, with the reference electrode used solely for controlling the potential of the working electrode, as most analytes are not electroactive. Electrochemical mediators are utilized for the analyte reaction at the working electrode. The potentiostat measures the potential difference between the reference electrode and the working electrode, allowing current to flow through the counter electrode and measuring the current as a voltage drop (IR) across a series resistance (R.m) [7]. Recently, flexible and wearable structures of enzyme-based bio-sensors have been introduced, which have many applications in these fields [8-10].

This paper presents a third-generation structure that enhances sensor sensitivity due to increased electrode contact surface with the analyte. The surface area is enhanced through the fabrication of interdigitated working electrodes and the growth of arrays of zinc oxide nanostructures. This configuration increases the number of redox reactions between the analyte and the working electrode, resulting in higher current density, improved sensitivity, and greater precision of the biosensor. Direct synthesis of zinc oxide via low-temperature hydrothermal growth not only increases the surface-to-volume ratio but also, due to its biocompatibility and high electron transfer rate, renders the electrochemical cell independent of mediators, thereby enhancing the potential, stability, and enzyme immobilization of the biosensor.

2. EXPERIMENTAL SECTION

2.1. Method and Material

In this paper, various materials were utilized for the electrode coating, including gold targets for electrode deposition, ammonium cerium nitrate ($Ce(NH_4)_2(NO_3)_6$), zinc nitrate tetrahydrate ($Zn(NO_3)_2$) from Merck, Hexamethylenetetramine (HMTA: $(CH_2)_6N_4$) from Merck, Zinc acetate dehydrate(ZAD: $Zn(CH_3CO_2)_2.2H_2O$) from Merck, Methylethylamine (MEA:C_3H_9N), sodium acetate trihydrate ($CH_3COONa.3H_2O$) from Merck, and Ag/AgCl ink from the Japanese company ALS. Additionally, powdered glucose oxidase enzyme was sourced from Sigma-Aldrich. The required equipment includes a thermal evaporation deposition system, a sputtering deposition system, a spin coater, a lithography system, an oven, a high-temperature furnace, a homogenizer, a potentiostat from Dropsense, an automatic injector, and a FE-SEM microscope utilized for the experiments conducted in this paper.

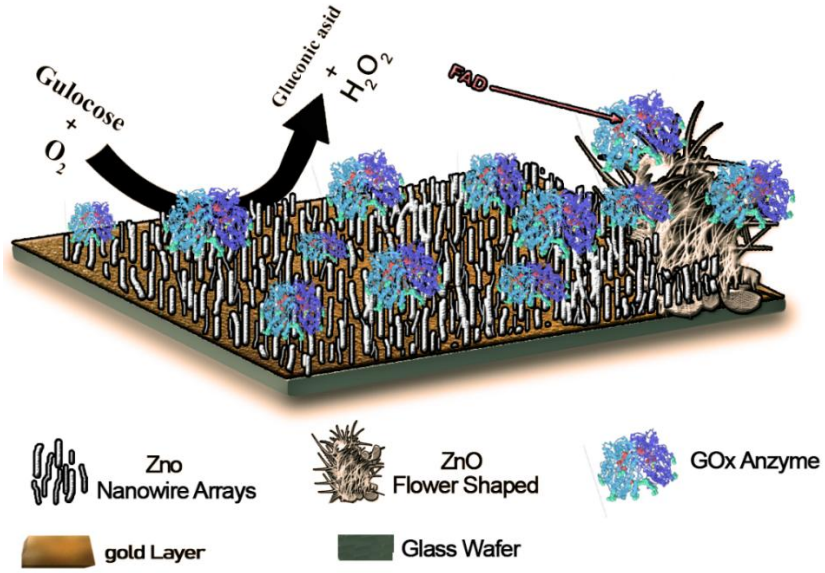

Figure 2. Schematic representation of the sensor electrode surface and the reaction of glucose with oxygen in the presence of the enzyme

2.2. Sensing mechanism

When a specific and appropriate volume of solution is injected into the sensor cell, the glucose present in the solution interacts with the biosensor, which has been coated with the enzyme.

The glucose oxidase enzyme facilitates the electrochemical reaction wherein glucose reacts with oxygen in the presence of glucose oxidase, producing hydrogen peroxide as a product of the biochemical process. Figure 2 provides a schematic representation of this reaction.

Oxidation/Reduction Reactions in Glucose Detection Oxidation/reduction (redox) reactions proceed as follows:

$$glu\,\mathrm{cos}e + O_2 \xrightarrow{glu\,\mathrm{os}eoxidase} glu\,\mathrm{c}onicacid + H_2O_2 \quad (1)$$

In another reaction, hydrogen peroxide decomposes, resulting in the release of electrons.

$$H_2O_2 \rightarrow O_2 + 2H^+ + 2e^- \quad (2)$$

The hydrogen ions react with oxygen to produce water.

$$O_2 + 4H^+ + 4e^- \rightarrow 2H_2O \quad (3)$$

The electrons from the oxidation/reduction reactions are transferred at the electrode interface by zinc oxide nanostructures, and the current resulting from the redox process is measured using a potentiostat. Since the number of chemical reactions involving glucose corresponds in a one-to-one ratio with the electrons generated from the redox reactions of hydrogen peroxide, we can relate the amount of electrons produced from the decomposition of hydrogen peroxide to the quantity of glucose present

Additionally, the following reactions occur alongside the reference electrode to maintain a constant potential.

$$AgCl + e \rightarrow Ag + Cl^- \quad (4)$$

$$Ag \rightarrow Ag^+ + e \quad (5)$$

$$Ag^+ + Cl^- \rightarrow AgCl \quad (6)$$

Therefore, according to the amperometric method, the potentiostat establishes a stable potential between the two reference and working electrodes, allowing for the measurement of current between the counter and working electrodes.

2.3. Glucose oxidase for glucose sensing

Glucose oxidase has been chosen for glucose detection sensors due to its high specificity for glucose and its production of hydrogen peroxide as a by-product. This enzyme serves as the primary basis for signaling in the sensor. Its stability and good performance under various conditions, particularly in aqueous environments, make it highly suitable for glucose sensors,

significantly enhancing the sensor's accuracy and sensitivity. Glucose oxidase facilitates the electrocatalytic reaction of glucose with oxygen, resulting in the production of glucolactone and hydrogen peroxide. The optimal pH for the enzyme's activity ranges from 5 to 5.5. As this reaction produces glucolactone and alters the pH of the environment, Tampon buffer solutions are employed to maintain a stable pH. This buffer also supports ionic interactions between the enzyme and the surface of the zinc oxide nanostructures by preserving appropriate ionic capacity, which aids in enzyme stabilization and improves sensor performance. According to the enzyme catalog purchased from Sigma, an appropriate buffer for the enzyme consists of 1 mg/mL of enzyme powder in a 0.05 M sodium acetate solution with a pH of 5, resulting in good enzyme efficacy.

2.4. Electrode fabrication

The sensor is constructed from three electrodes. Figure 3 illustrates the schematic and dimensions of the mask, including the spacing between the electrodes to use in the electrode fabrication process on a glass substrate.

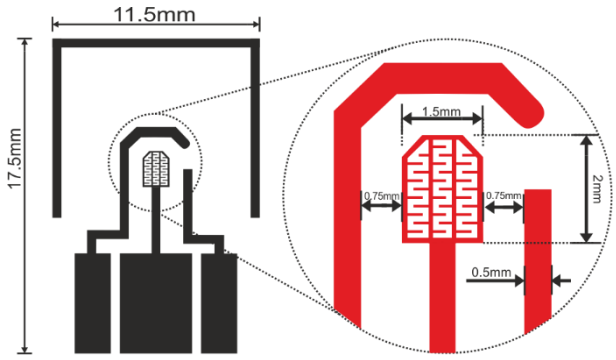

Figure 3. Schematic representation of electrode design of the electrochemical glucose sensor and its dimensions

2.5. Electrode modification using zno nanostructures

Modification of the Working Electrode: after the deposition and patterning of the electrode, zinc oxide nanostructures and a nanowire/flower-like structure combination are created on the working electrode to enhance sensor performance. Two methods of utilizing zinc oxide nanostructures are employed: in the first method, zinc oxide nanostructures are grown on the working electrode using a hydrothermal growth method, while in the second method, after the growth of ordered nanostructures, a solution containing flower-like zinc oxide nanostructures is added to this electrode. Hydrothermal growth results in an aligned morphology. For creating a composite structure (nanostructures combined with flower-like structures), in addition to growing nanowires in the growth solution, a separate solution containing flower-like zinc oxide

nanostructures is synthesized and added to the grown nanowires. The hydrothermal method is a suitable, rapid, and cost-effective approach for synthesizing zinc oxide nanostructures, allowing for the easy fabrication of denser structures. To selectively grow zinc oxide nanostructures on the working electrode, a laser-cut PET mask is used.

Modification of the Reference Electrode: For the modification of the reference electrode, the upper part of the reference electrode, with an area of 1.5 mm^2, is coated with a prepared Ag/AgCl solution using a screen-printing technique. After deposition, the solution is allowed to stabilize on the electrode.

2.6. Hydrothermal growth of zinc oxide nanostructures

Nano-Structures: the growth of nanostructures via the hydrothermal method is performed in two stages: the first stage involves the nucleation process. For this purpose, 0.2 g of zinc acetate dihydrate is mixed with 25 mL of ethanol and 0.5 mL of methyl ethyl amine for 15 minutes. Methyl ethyl amine is used to enhance the solubility of zinc acetate in water and aids in forming a matrix containing zinc sources. An aluminum foil is then placed over the mixture, and after two days, a viscous gel containing zinc sources is obtained. This resultant matrix is deposited using a stencil with an automatic injection system and subsequently dried at 100^{o}C. The deposition and drying processes are conducted in three stages to achieve the desired nucleation density. Following the seeding process, the sample is annealed at 300^{o}C. The second stage involves preparing the growth solution. Initially, 100 mL of DI water is mixed with 0.62 g of zinc nitrate tetrahydrate and 0.34 g of hexamethylenetetramine for 25 minutes on a stirrer until a clear solution is obtained. The beaker containing the growth solution is placed inside a tall glass container of small diameter, and the sample is positioned within it such that the growth surface faces upward. After sealing, the sample is placed in an oven at 117^{o}C for six hours. After the growth of the nanostructures, the sample is removed and placed on a hot plate to dry. The sample is then placed in a furnace at 400^{o}C to create a homogeneous structure and remove any excess organic material. This process also enhances the crystallinity of the structure.

Flower-like Nanostructures: To synthesize the flower-like zinc oxide nanostructures, 0.09 g of hexamethylenetetramine is dissolved in 25 mL of DI water in a 50 mL beaker using a stirrer at 45 degrees Celsius for 15 minutes. In another beaker, 0.15 g of zinc nitrate tetrahydrate is dissolved in 25 mL of DI water under the same temperature and time conditions. The two solutions, along with 0.7 mL of ammonia, are stirred at 50 degrees Celsius for 10 minutes. The resultant solution is then placed in a 150 mL glass container and heated in an oven at 120^{o}C for 7 hours. After the formation of zinc oxide nanostructures, to enhance selectivity in the sensor and increase reaction rates, glucose oxidase enzyme is injected as a solution in sodium acetate buffer onto the porous zinc oxide substrate. This creates a flower-like structure of the zinc oxide nanostructures on the electrode, formed by the zinc oxide nanostructures.

2.7. Sensor integration

After constructing and modifying the electrodes with suitable solutions and nanostructures, the packaging testing stages ensue. Figure 4 illustrates the key steps involved in packaging this sensor.

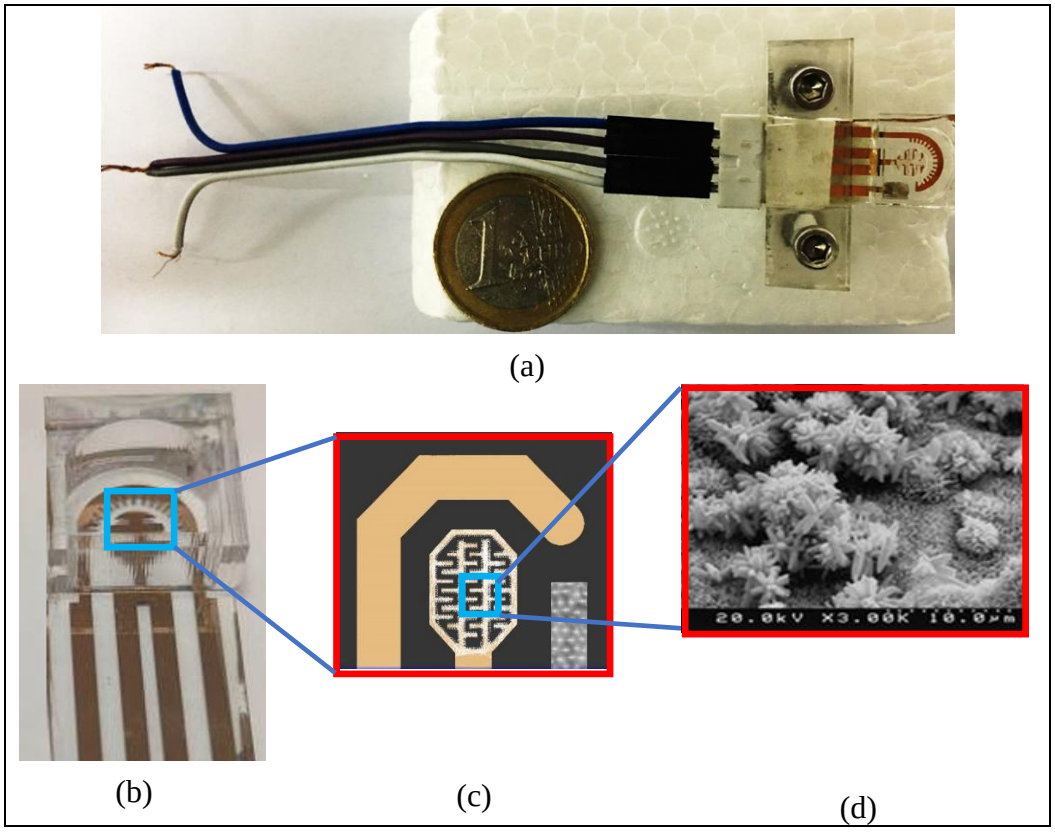

Figure 4. a) the final packaging of the sensor; b) integrated sensor; c) magnified view of the counter electrode; d) the multilayer ZnO nanostructures on the counter electrode

3. RESULTS AND DISCUSSION

3.1. Various Structure of Sensors

Three types of sensors are introduced and examined: 1) Sensor without ZnO Nanostructures: this sensor features the typical shape of electrodes and is evaluated without zinc oxide nanostructures to assess the quality of the electrodes. 2) Sensor with Zinc Oxide Nanostructures: this sensor is constructed with the standard electrode configuration. Zinc oxide nanostructures are grown on the working electrode using the hydrothermal method, followed by the droplet application of a sodium acetate buffer solution containing glucose oxidase enzyme onto the nanostructures. 3) Sensor with Zinc Oxide Nanostructures and Multi-dimensional Flower-like Structure: this sensor maintains the conventional electrode structure, where zinc oxide nanostructures are grown on the working electrode via the hydrothermal

method. Subsequently, a pre-prepared solution containing flower-like zinc oxide nanostructures is added to these nanostructures using the injection method.

3.2. Zinc Oxide Nanostructure Synthesis

The growth of zinc oxide nanostructures is conducted using solutions of zinc nitrate and hexamethylenetetramine (hexamine). Hexamine reacts with water to produce formaldehyde and ammonia, leading to the formation of zinc oxide nanostructures. It is noteworthy to mention that there are other physical and green processes for ZnO nanorod synthesis, which can be more effective in mass-scale production at low and high temperatures [11-15]. Figure 5 presents the FE-SEM images related to the nanostructures on the working electrode, which were achieved through a growth process in the synthesis solution

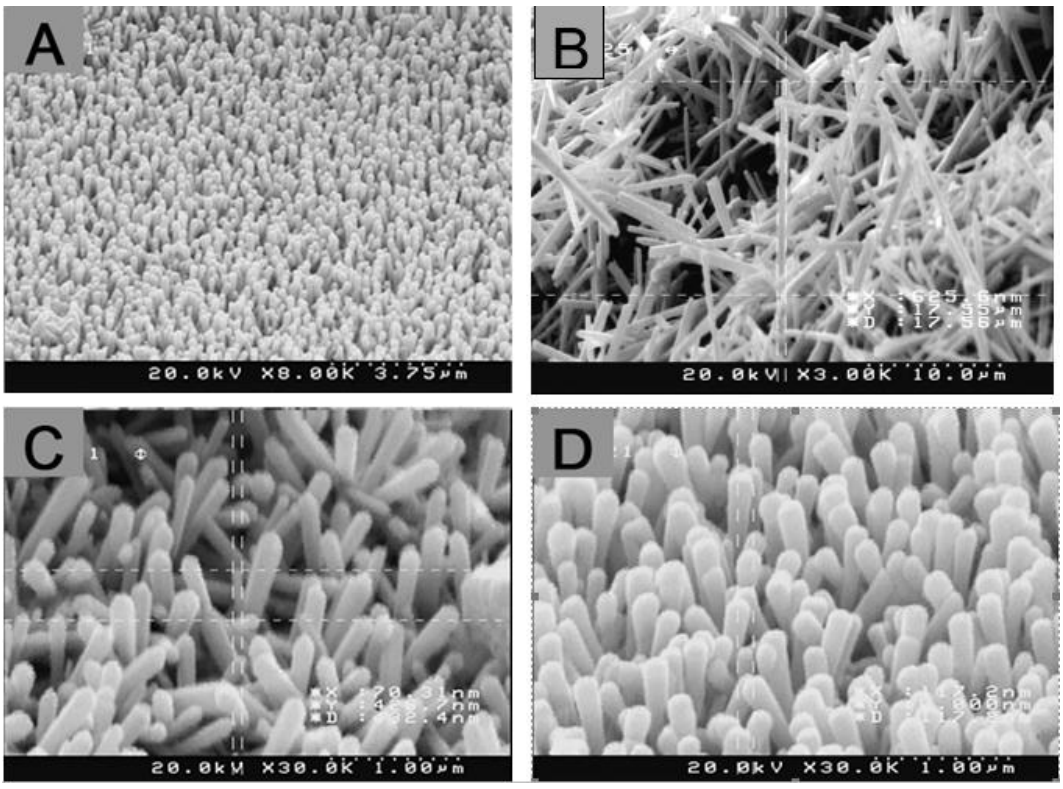

Figure 5. FE-SEM images of the growth of ZnO nanostructure arrays on the working electrode; A, C, and D show the nanostructures grown on a sensor directly and B shows the nanostructures injected into the working electrode using the micro-injection setup (the average diameters of approximately 70 nm and lengths of 1.5 μm)

As observed, the size of the nanostructures is nearly uniform. As expected, the grain growth in a gel-like matrix on the electrodes results in an arrayed and organized growth of the nanostructures. In contrast, the nanostructures formed by dripping the solution onto the electrodes exhibit less arrayed organization. The length of the grown nanostructures ranges

from 1.2 µm to 1.5 µm, with diameters varying from approximately 50 nm to 120 nm. Following the growth of these nanostructures, 0.1 mL of the solution containing flower-like nanostructures is dripped onto the nanostructures to enhance the active surface area. The branches of the flower-like zinc oxide structures measure around 2.5 µm in length, with a diameter of approximately 500 nm. Figure 6 shows the FE-SEM images of the flower-like structures deposited onto the nanostructures created through the nanowire growth process.

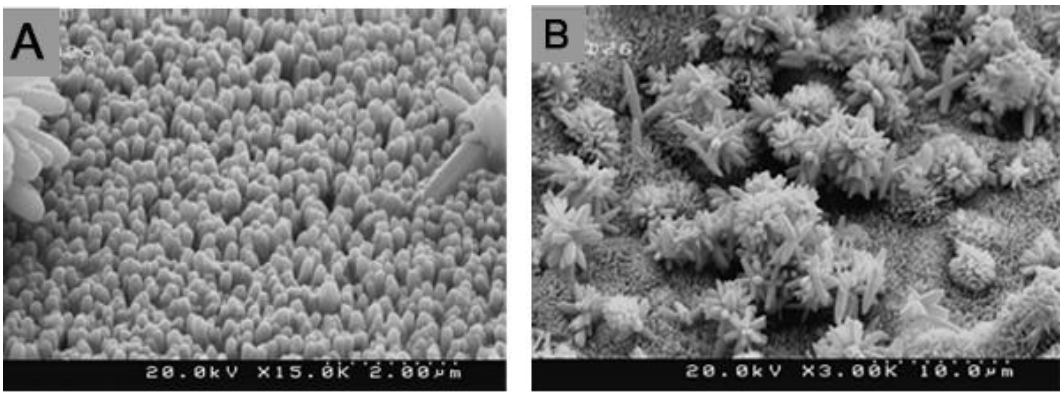

Figure 6. FE-SEM images of the growth of zinc oxide dual structures: A and B) flower-like structures and nanowires (nanowire, flower-like nanostructure) at different magnifications of X15 and X3

3.3. Cyclic voltammetry test

After constructing the electrochemical glucose sensors, the cyclic voltammetry (CV) of the sensors was tested using a potentiostat. For this purpose, a specialized glucose serum solution for glucose measurement tests was purchased from a biochemical company. In cyclic voltammetry, the potentiostat applies a linear voltage over a specified range (for example, from 0 to 0.8 volts versus the Ag/AgCl electrode). On the surface of the working electrode, glucose is broken down by glucose oxidase, resulting in the production of hydrogen peroxide. At an appropriate voltage (overvoltage), a redox reaction involving hydrogen peroxide occurs, leading to either electron generation or consumption. This reaction generates a current peak in the cyclic voltammetry (CV) curve, which can be analyzed based on its voltage position and current intensity.

The sensitivity of the sensor is defined as follows:

$$Sensitivity = \frac{\text{Changes in current intensity in both analyte and non} - \text{analyte conditions}}{The\ surface\ area\ of\ electrode \times glucose\ concentration} \quad (7)$$

The surface area of the electrode is equal to 0.03 cm², and the glucose concentration is 2.1 mg/mL=11.66mM/l.

In the initial step of sensor evaluation, it is essential to determine whether the redox processes occur completely on the sensor, independent of the type of analyte and enzyme. Furthermore, it is important to ensure that the voltage application, electron transfer, and accurate current reading function effectively. For this purpose, the reference solution $[Fe(CN)6]^{3-/4-}$ is used. This substance provides a cyclic voltammetric response with any amperometric electrochemical sensor, serving as an indicator of the electrodes' proper functioning. A satisfactory response to this solution indicates that the electrochemical sensor electrodes, including the working, reference, and counter electrodes, are operating correctly, thereby allowing the use of enzymes and other materials. Cyclic voltammetry of the reference solution $Fe(CN)6]^{3-/4-}$ performed well, with oxidation and reduction occurring effectively at a scan rate of 200 mV/s, resulting in distinguishable peaks (Figure 7). During the forward scan at a voltage of 0.46 V, a current peak of 88.7 µA is observed, and during the return cycle at a voltage of -0.38 V, a current peak of -58.25 µA is recorded.

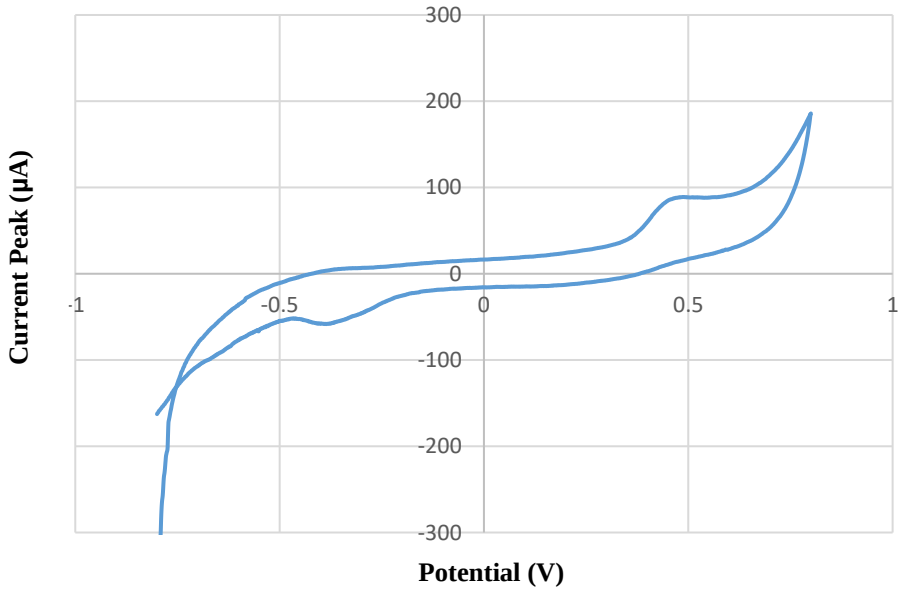

Figure 7. Suitable cyclic voltammetry responses to $[Fe(CN)_6]^{3-/4-}$ on the electrodes prior to the deposition of zinc oxide nanostructures and glucose oxidase, at a scan rate of 200 mV/s

First structure: In this sensor, no zinc oxide nanostructures are deposited on the working electrode; instead, glucose oxidase is immobilized onto a gold layer on the working electrode. The cyclic voltammetry (CV) of this sensor is investigated under two different conditions: in the absence of the analyte (at a scan rate of 200 mV/s) and in the presence of the analyte (with varying scan rates of 50, 100, and 200 mV/s). Figure 8 presents the results obtained from this sensor. The current peak in the absence of the analyte, measured at a scan rate of 200 mV/s, is recorded at a voltage of 0.25 V, yielding a reduction half-cycle current of 2.4 µA. In the presence of the analyte (glucose at a concentration of 2.1 mg/ml), the current peaks at scan rates of 200 mV/s, 100 mV/s, and 50 mV/s occur at voltages of 0.32 V, 0.26 V, and 0.25 V,

respectively, producing current values of 5.71 µA, 4.7 µA, and 3.9 µA. No significant peak was observed in the reduction half-cycle. According to equation (7) the sensitivity of the sensor is determined to be 9.45 $\mu AmM^{-1}cm^{-2}$. The sensor response in the reduction half-cycle was recorded over a duration of 7 seconds.

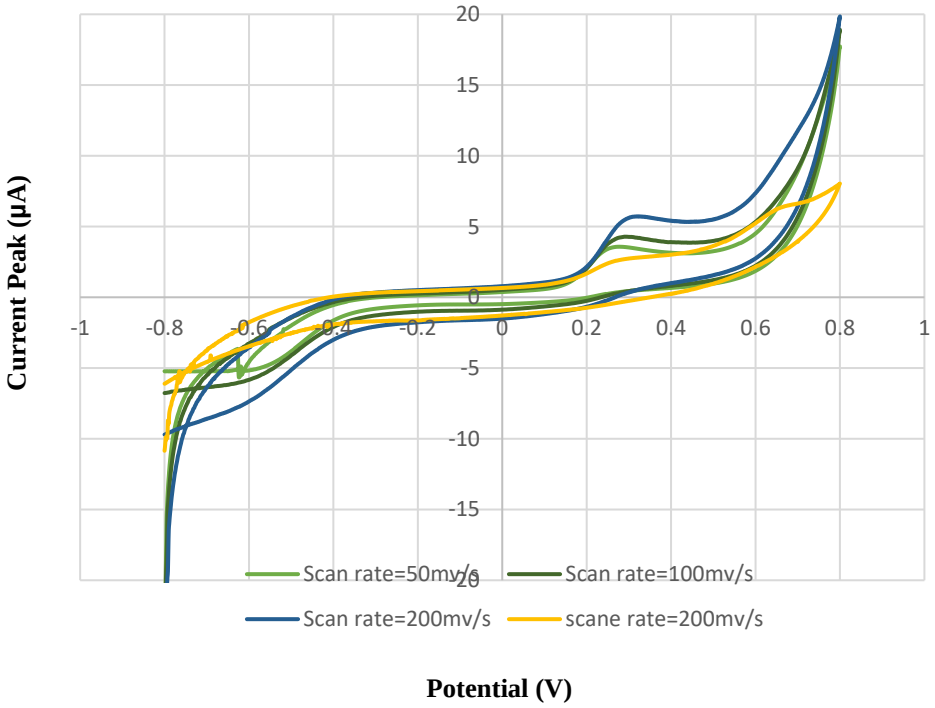

Figure 8. CV cycles for the biosensor without zinc oxide structure in two conditions: without analyte (at a scan rate of 200 mV/s) and with analyte (at varying scan rates of 50, 100, and 200 mV/s)

Second structure: the performance evaluation of glucose sensor electrodes, which feature a standard electrode configuration with glucose oxidase enzyme immobilized on the zinc oxide structure, was carried out. This assessment took place before the zinc oxide and enzyme coating. Figure 9 illustrates the cyclic voltammogram of the sensor containing zinc oxide nanowires at a glucose concentration of 2.1 mg/mL. Initially, the electrolyte without analyte (glucose) was tested, and the desired electrolyte solution, a sodium acetate buffer containing 2 mg/mL of the enzyme, was injected into the electrochemical cell holder in a volume of 0.3 mL. In the CV cycle without analyte, a current peak of 9.7 µA was observed during the reduction at a voltage of 0.46 V, and during oxidation, a current intensity of -16.9 µA was measured at a voltage of -0.65 V, indicating that the nanostructures influence direct electron transfer. Referring to the CV plots for the biosensor with zinc oxide nanostructures, a current peak of 48.65 µA was noted during the reduction at a voltage of 0.26 V, and during oxidation, a current peak of -62.71 µA was recorded at a voltage of -0.60 V. According to the equation (7) the sensor's sensitivity was calculated to be 13.63 $\mu AmM^{-1}cm^{-2}$.

Since the LSV and CV diagrams at a constant scan rate are nearly identical, this indicates the sensor's stability. The half-cycle duration for both the forward and return paths was 6 seconds, thereby evaluating the sensor response time, which typically exhibits greater stability during the return half-cycle, also at 6 seconds.

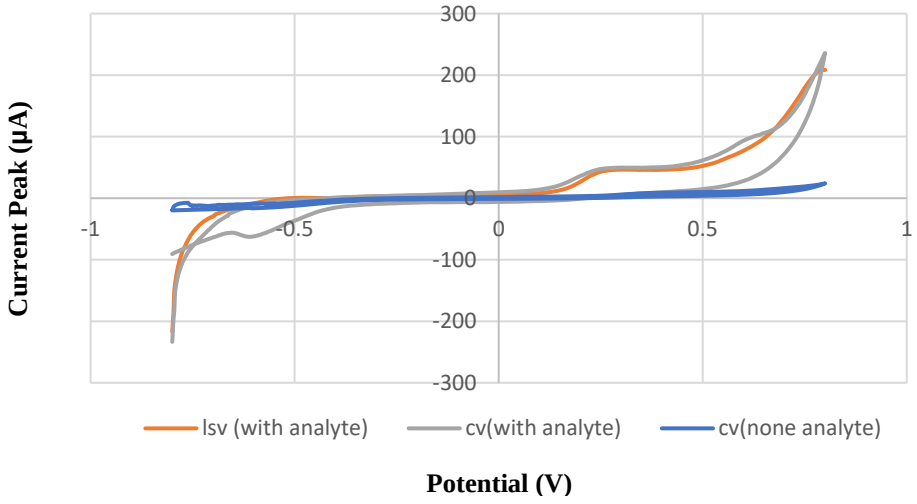

Figure 9. CV and LSV cycles for the biosensor with zinc oxide nanostructures and glucose oxidase enzyme, with and without analyte at a scan rate of 100 mV/s

Third structure: The cyclic voltammetry of the glucose sensor containing zinc oxide nanostructures and flower-like structures was tested at scan rates of 50, 100, 150, and 200 mV/s. Figure 10 presents the cyclic voltammetry of this biosensor .

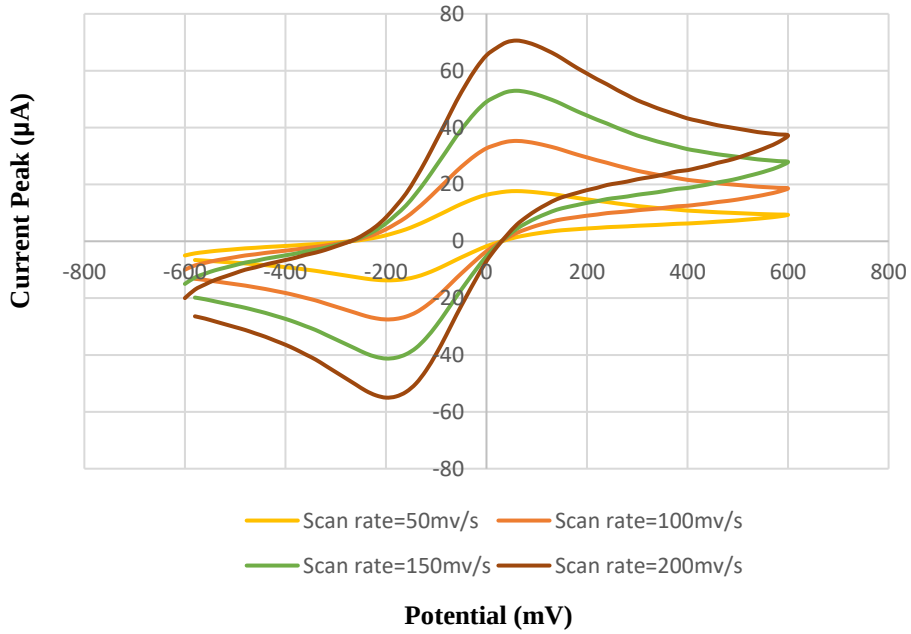

Figure 10. Voltammetric cycles of the glucose biosensor at scan rates of 50, 100, 150, and 200 mV/s

The diagram indicates that the response is complete; as the scan rate increases, the current is observed to double exactly, demonstrating a linear response of the sensor to the voltage (with a correlation coefficient equal to one). The cyclic voltammetry shows that at scan rates of 50, 100, 150, and 200 mV/s, the cathodic current peak values during the first half-cycle at a voltage of 60 mV are 70.06, 52.95, 35.3, and 17.65 µA, respectively. In the anodic half-cycle at a voltage of -200 mV, the current peak values are -13.75, -27.5, -41.25, and -55 µA, respectively. The symmetry of the cyclic voltammetry indicates that the oxidation and reduction reactions occur equally and that the reactions are controlled. Additionally, at relatively low potentials, a relatively large current peak is observed. As the scan rate increases, both anodic and cathodic peaks increase at a constant ratio, implying a relationship between the anodic and cathodic peaks. The diagram demonstrates the process is controlled by the adsorption of redox species, with enhanced stability of the enzyme immobilized on the electrode surface and rapid electron transfer.

The potential range of the forward and reverse peaks (-0.2 to 0.2 volts) indicates that the zinc oxide nanostructures reduce the overvoltage for the redox reactions of hydrogen peroxide. Selecting this optimal range (-0.2 to 0.2 volts) minimizes the interference of electroactive species, thus enhancing the selectivity of the sensor. The response time of the sensor was measured at 7.1 seconds for the forward path and 5.9 seconds for the return path, resulting in an estimated response time of 7.1 seconds. According to equation (7) the sensitivity of the sensor was determined to be 21.12 $\mu AmM^{-1}cm^{-2}$. Figure 11 illustrates the relationship between scan rate and current, indicating a linear relationship between the scan rate and the peak currents of both the anodic and cathodic processes.

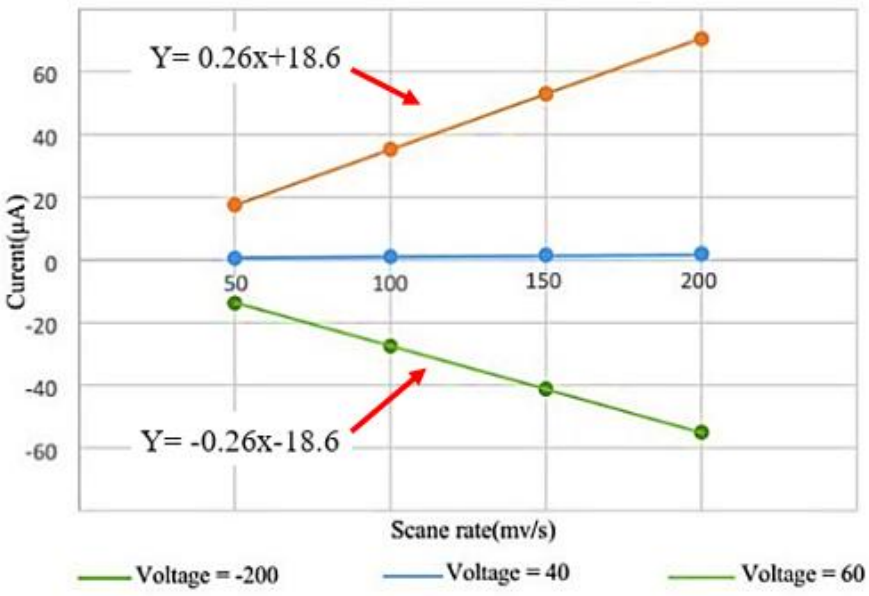

Figure 11. Linear variation of the amperometric response of the glucose sensor with increasing scan rates at voltages of 40 mV, 60 mV, and -200 mV

The linear equation relating the scan rate to the cathodic current peaks is given by:

$$Y= 0.26x+18.6 \quad (8)$$

And the equation for the anodic current peaks is as follows:

$$Y= -0.26x-18.6 \quad (9)$$

Figure 12 presents the chronoamperometric response of the sensor with the nanowire/flower-like zinc oxide structure. According to the chronoamperometric diagram, the sensor's response to a glucose concentration of 2.1 mg/mL indicates that at 10.2 seconds, the current is 11.83 µA. It is observed that for a duration of 0.1 seconds, the current decreased from 11.83 µA to -5.45 µA. The structures based on the growth of nanostructures and the deposition of flower-like zinc oxide nanostructures possess a higher surface-to-volume ratio, allowing for more enzyme loading on the substrate, and facilitating the reactions. The presence of a very low baseline current and sharp, narrow peaks indicates that within a very low potential range in the optimal zone (-0.2 to 0.2 volts against Ag/AgCl), the interference of electroactive elements is reduced, enhancing selectivity and accuracy of the sensor. A correlation coefficient of one signifies very high sensor stability, as the current also doubles with a doubling in the scan rate.

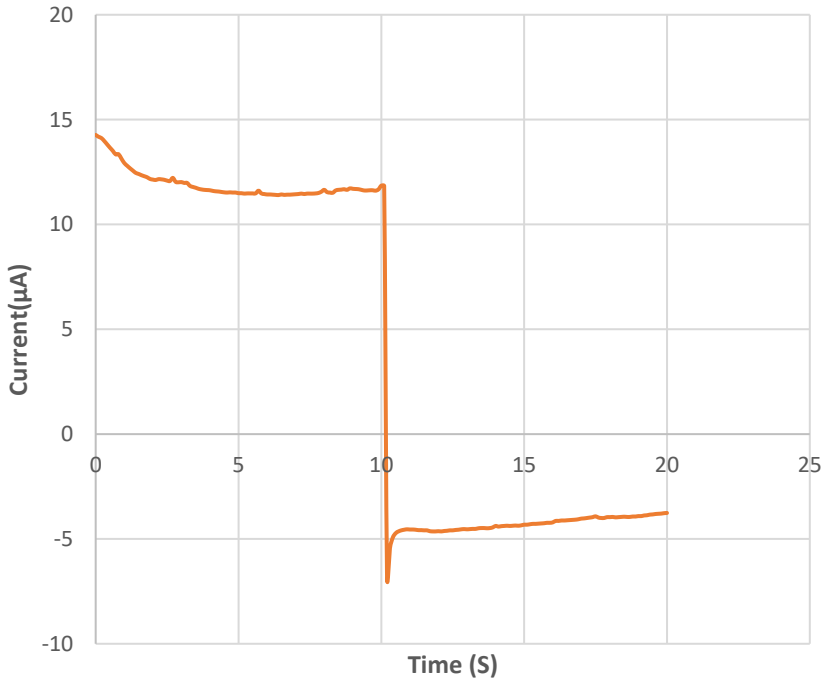

Figure 12. Chronoamperometric diagram of the glucose sensor based on flower-like/zinc oxide nanowire structures

Table 1 compares this sensor with other similar sensors. As observed, the specifications of this sensor have improved compared to other sensors.

Table 1. Comparison of different research groups' outstanding similar sensors

Report	Description	Linear Measuring Range	Limit of Detection	Sensitivity	Ref.
Proposed structure	Multi-layer ZnO-nanostructures/Ag	0.002–10 mM	2 µM	21.12 $\mu AmM^{-1}cm^{-2}$	This work
Yu Zhao et al, 2016	ZnO-nanorods/graphene heterostructure for direct electron transfer between GOx and Electrode	0.2–1.6 mM	Not Given	17.64 μAmM^{-1}	[16]
Wang AJ et al, 2012	Non-enzymatic electrochemical sensing of glucose with Cu/Cu2O HMs modified electrode	0.22–10.89 mM	0.05 µM	33.63μAmM^{-1}	[4]
Xiao Li, et al, 2015	A paper-based microfluidic biosensor integrating zinc oxide nanowire	0−15 mM	59.5 µM	8.24 $\mu AmM^{-1}cm^{-2}$	[17]
F. Shi, J. Xu et al, 2021	Bird nest-like zinc oxide (BN-ZnO) nanostructures to develop a sensitive electrochemical glucose biosensor	0.005-1.6 mM	0.004 mM	15.6 $mAM^{-1}cm^{-2}$	[18]
Natalija German et al, 2014	Enzymatic (GOx) Glucose Biosensor Gold Nanoparticle on graphite rod	0.1–10 mM	0.083 mM	101.02 $AmM^{-1}cm^{-2}$	[19]
Siva Kumar-Krishnan et al, 2013	Chitosan supported AgNWs Enzymatic Glucose Biosensing	1-15 mM	Not Given	16.72 $\mu AmM^{-1}cm^{-2}$	[20]
Adil Emin et al, 2024	poly(ProDOT-$(MeSH)_2$)/Au/rGO composite non-enzymatic glucose biosensors	0.04–16.0 mM	0.01 µM	46.13 $\mu AmM^{-1}cm^{-2}$	[21]

4. CONCLUSION

In the second generation, intermediates are oxidized or reduced, which enhances electron transfer; however, the use of intermediates also increases the overpotential. This challenge is addressed using zinc oxide nanostructures, which leverage hydrogen peroxide for detection, thus alleviating the issue. Zinc oxide nanostructures do not need to connect to the active center of the enzyme; instead, they serve merely as a medium for enzyme stabilization and act as a platform for the electron transfer resulting from the redox process of hydrogen peroxide. In this mechanism, they do not participate in the sensing process directly and function exclusively as electron transfer intermediates, which prevents any increase in overpotential. The maximal anodic current peak achieved is approximately 70.6 µA at a scan rate of 200 mV/s for a glucose concentration of 2.1 mg/dL. The voltage response in comparison to other biosensor samples is considered low, resulting in significant current generation even at low potentials. This enzyme is well-suited for glucose sensors due to its stability and good performance under various conditions, especially in aqueous environments, significantly enhancing the accuracy and

sensitivity of the sensor. The utilization of the nanostructures/flower-like structure of zinc oxide increases the surface-to-volume ratio and electron transfer capacity, accommodating higher amounts of enzyme immobilization. This improved structure facilitates the stabilization of glucose oxidase. The high electron transfer rate leads to a substantial reduction in overpotential for the hydrogen peroxide redox process, with the working potential set in the optimal range (-0.2 to 0.2 volts *vs*. Ag/AgCl) effectively minimizing interference from electroactive elements, resulting in enhanced selectivity and improved linearity of the sensor. Consequently, this approach yields higher sensitivity. Additionally, the superhydrophilic nature of zinc oxide nanostructures promotes rapid glucose sample adsorption, further increasing sensor sensitivity.

Acknowledgments

Sincere gratitude is hereby given to Dr. Hosseini for providing us with the test equipment at the Electrochemistry Institute of the University of Tehran.

Declarations of interest

The authors declare no conflict of interest in this reported work.

REFERENCES

[1] A. Emin, A. Ding, and H.S. Ali, Microchem. J. 207 (2024) 111972.
[2] J. Wang, Electrochemical Sensors, Biosensors and their Biomedical Applications, Elsevier (2008) pp. 57–69.
[3] J. Wang, Analytical Electrochemistry, Third Edition, Wiley (2006).
[4] J. Wang, Chem. Rev. 108 (2007) 814.
[5] M. Zayats, J. American Chem. Soc. 127 (2005) 12400.
[6] C.M. Wong, K.H. Wong, and X.D. Chen, Applied Microbiol. Biotech. 78 (2008) 927.
[7] D. Grieshaber, R. MacKenzie, J. Vörös, and E. Reimhult, Sensors 8 (2008) 1400.
[8] S. Moradi, A. Firoozbakhtian, M. Hosseini, O. Karaman, S. Kalikeri, G.G. Raja, and H. Karimi-Maleh, Int. J. Biological Macromolecules 254 (2024) 127577.
[9] A. Atefi, S. Moradi, F. Salehnia, and M. Hosseini, Microchem. J. 209 (2025) 112809.
[10] Z. Damirchi, A. Firoozbakhtian, M. Hosseini, and M.R. Ganjali, Microchim. Acta 191 (2024) 06209.
[11] M.K. Tabatabaei, H.G. Fard, J. Koohsorkhi, Nano 10 (2015) 1550040.
[12] M.M.H. Shahkarami, J. Koohsorkhi, H. GhafooriFard, Nano 12 (2017) 1750044.
[13] S. Karthik, P. Siva, K.S. Balu, R. Suriyaprabha, V. Rajendran, and M. Maaza, Advanced Powder Technology 28 (2017) 3184.
[14] H.G. Fard, J. Koohsorkhi, J. Mohammadnejad Arough, IET nanobiotechnology 14 (2020) 126.
[15] J. Koohsorkhi, S. Sanjari and M. Kafi, Anal. Bioanal. Electrochem. 16 (2024) 315.
[16] Y. Zhao, W. Li, L. Pan, J. Scientific Reports (2016) Art. 32327.

[17] X. Li, C. Zhao, and X. Liu, Microsystems & Nanoengineering 1 (2015) 15014.
[18] F. Shi, J. Xu, Z. Hu and et al., Chinese Chem. Lett. 32 (2021) 3185.
[19] N. German, A. Ramanavicius, and A. Ramanaviciene, Sens. Actuators B: Chemical 203 (2014) 25.
[20] K. Krishnan, RSC Advances 6 (2016) 20102.
[21] A. Emin, A. Ding, and H.S. Ali, Microchem. J. 207 (2024) 111972.